# Voltage-dependent Block of Anthrax Toxin Channels in Planar Phospholipid Bilayer Membranes by Symmetric Tetraalkylammonium Ions

## *Single-Channel Analysis*

ROBERT O. BLAUSTEIN, E. J. A. LEA, and ALAN FINKELSTEIN

From the Departments of Physiology & Biophysics and Neuroscience, Albert Einstein College of Medicine, Bronx, New York 10461; and School of Biological Sciences, University of East Anglia, Norwich NR4 7TJ, United Kingdom

ABSTRACT Previous studies have shown that symmetric tetraalkylammonium ions affect, in a voltage-dependent manner, the conductance of membranes containing many channels formed by the $PA_{65}$ fragment of anthrax toxin. In this paper we analyze this phenomenon at the single-channel level for tetrabutylammonium ion ($Bu_4N^+$). We find that $Bu_4N^+$ induces a flickery block of the $PA_{65}$ channel when present on either side of the membrane, and this block is relieved by large positive voltages on the blocking-ion side. At high frequencies (>2 kHz) we have resolved individual blocking events and measured the dwell times in the blocked and unblocked states. These dwell times have single-exponential distributions, with time constants $\tau_b$ and $\tau_u$ that are voltage dependent, consistent with the two-barrier, single-well potential energy diagram that we postulated in our previous paper. The fraction of time the channel spends unblocked $[\tau_u/(\tau_u + \tau_b)]$ as a function of voltage is identical to the normalized conductance-voltage relation determined from macroscopic measurements of blocking, thus demonstrating that these single channels mirror the behavior seen with many (>10,000) channels in the membrane. In going from large negative to large positive voltages (−100 to +160 mV) on the *cis* ($PA_{65}$-containing) side of the membrane, one sees the mean blocked time ($\tau_b$) increase to a maximum at +60 mV and then steadily decline for voltages greater than +60 mV, thereby clearly demonstrating that $Bu_4N^+$ is driven through the channel by positive voltages on the blocking-ion side. In other words, the channel is permeable to $Bu_4N^+$. An interesting finding that emerges from analysis of the voltage dependence of mean blocked and unblocked times is that the blocking rate, with $Bu_4N^+$ present on the *cis* side of the membrane, plateaus at large positive *cis* voltages to a voltage-independent value consistent with the rate of $Bu_4N^+$ entry into the blocking site being diffusion limited.

Address reprint requests to Dr. Alan Finkelstein, Department of Physiology and Biophysics, Albert Einstein College of Medicine, 1300 Morris Park Ave., Bronx, NY 10461.

J. GEN. PHYSIOL. © The Rockefeller University Press · 0022-1295/90/11/0921/22 $2.00 921
Volume 96 November 1990 921–942

## INTRODUCTION

In the preceding paper (Blaustein and Finkelstein, 1990*a*) we described the voltage-dependent effects of symmetric tetraalkylammonium ions (tetramethylammonium through tetrahexylammonium) on the macroscopic conductance induced in planar phospholipid bilayer membranes by the $PA_{65}$ fragment of anthrax toxin. Although the membranes contained hundreds or thousands of channels, we interpreted the effects of those ions on the "instantaneous" *I-V* or *g-V* characteristics as resulting from their ability to block ion flow through the channel. The simplest interpretation of our data was with a two-barrier, single-well model of the channel (Fig. 1), in which

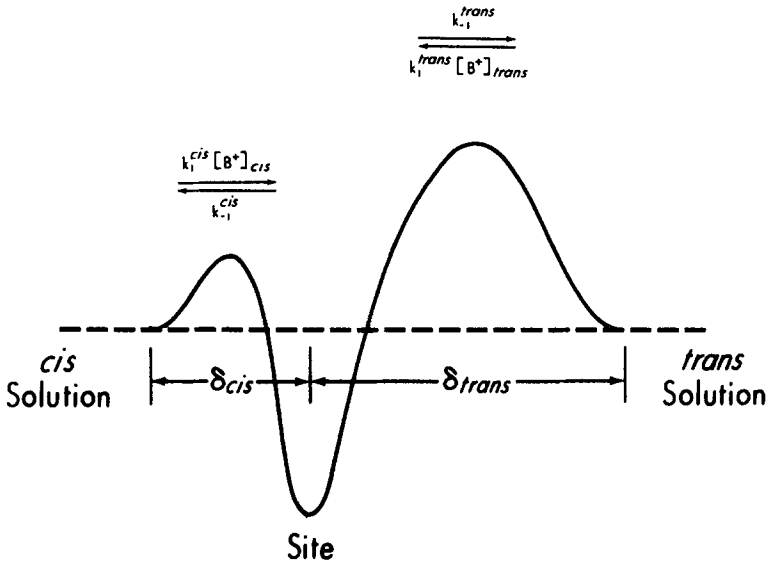


FIGURE 1. Free energy diagram (at $V = 0$) of the proposed energy barriers and well for tetraalkylammonium ions in a $PA_{65}$ channel. Note that the well is closer to the *cis* side and that the *trans* barrier is higher than the *cis* barrier. The rate constants for entering and leaving the well are also indicated. Since all experiments described in this paper were with the blocking ion ($B^+$) present on only one side of the membrane, only one of the entry processes is relevant; that is, with $B^+$ in the *cis* solution, $k_1^{trans}.[B^+]_{trans} = 0$, whereas with $B^+$ in the *trans* solution, $k_1^{cis}.[B^+]_{cis} = 0$.

occupancy of the well, or binding site, by a tetraalkylammonium ion blocks the conductance of the major current-carrying cation ($K^+$ at 100 mM in our experiments). The channel was presumed to be permeable to the blocking ion, thus accounting for the rise in conductance (i.e., relief of block) at large positive voltages on the blocking-ion side; the energy barrier near the *cis* side (the side to which $PA_{65}$ is added) was made smaller than that near the *trans* side to account for the greater effectiveness of blocker addition to the *cis* solution.

Although the model in Fig. 1 adequately accounts for the macroscopic data, those data do not provide a very stringent test of the model, and indeed it is conceivable

(albeit unlikely) that the effects of the tetraalkylammonium ions on the macroscopic *I-V* characteristics could result from a direct effect on channel gating that does not involve blocking and unblocking. Furthermore, even if one accepts a blocking mechanism, it is not obvious that the data are explicable by a single binding site within the channel (see Discussion), and in addition, no information about the individual rate constants in crossing the barriers is extractable from the macroscopic *g-V* curves. For these reasons we have examined the action of tetraalkylammonium ions on $PA_{65}$-treated membranes at the single-channel level. To this end we performed a detailed study of the effect of tetrabutylammonium ion ($Bu_4N^+$) on the $PA_{65}$ channel, in which we resolved the dwell times of the channel in the blocked and unblocked states. We find that the dwell times in these states are fit by single exponentials, and their voltage and concentration dependencies are consistent with a simple two-barrier, single-well model. In particular, the rate constant for exit from the blocked state does not depend on either the blocker concentration or the side to which blocker is added; in addition, it goes through a minimum (as a function of voltage), a finding consistent with the assumption that at appropriate voltages the blocker can exit the channel to the side opposite from which it entered. The entrance rate is directly proportional to blocker concentration, and our analysis also indicates that over a large part of the voltage range examined, the entrance rate of $Bu_4N^+$ from *cis* solution to the blocking site is diffusion limited.

## MATERIALS AND METHODS

### *Anthrax Toxin Preparation, Storage, and Addition*

Protective antigen (PA) of anthrax toxin was a generous gift from Dr. T. M. Koehler and Dr. R. J. Collier of the Department of Microbiology and Molecular Genetics, Harvard Medical School. The protein was purified and trypsin-cleaved, as previously described, to yield $PA_{65}$ (Blaustein et al., 1989) which was then stored in 0.35 M NaCl/20 mM ethanolamine HCl, pH 9.0, as frozen aliquots; once thawed it could be kept at 4°C at a concentration of ~600 μg/ml for several months. Fresh dilutions of $PA_{65}$ were made each week to concentrations of 50 μg/ml in 0.1 M KCl/1 mM EDTA, pH 7.5; before each experiment this solution was diluted to one of two concentrations: 5 μg/ml if toxin was added to the cup side (volume = 700 μl) of the bilayer, which had a large (several hundred microns) unstirred layer; or 50 ng/ml if toxin was added to the opposite side (volume = 3 ml). The compartments contained identical solutions of 0.1 M KCl/1 mM EDTA, pH 6.6, and could be stirred by small magnetic stir bars. After bilayers were formed (see below), ~10 μl of $PA_{65}$ solution was added to one compartment, which we define as the *cis* compartment. A single channel would usually appear after waiting 30 min to 2 h; all data were obtained on membranes containing only one channel.

### *Membrane Formation and Recording*

Planar diphytanoylphosphatidylcholine (DPhPC) phospholipid bilayer membranes were formed at room temperature across a 50-μm hole in a polystyrene cup. The techniques used to construct cups with this size hole were taught to us by Dr. W. F. Wonderlin of the Department of Physiology, University of Alberta, Alberta, Canada, and are explained in detail elsewhere (Wonderlin et al., 1990). Bilayer formation was accomplished using a modification (also suggested by Dr. Wonderlin) of the brush technique of Mueller et al. (1963). Approximately 1 μl of a 0.5% solution of DPhPC in pentane was blown over the hole (outside only) as a

"prepainting" step; membranes were "painted" by brushing a small quantity of a 3% solution of DPhPC in *n*-decane over the hole. Membranes thus formed typically had a capacitance, when thinned, of ~20 pF (including an intrinsic cup capacitance of ~5 pF) and a rms noise level (3–3,000 Hz) of ~0.5 pA. Membranes were also electrically "tight" ($g < 5$ pS) and quite stable, lasting several hours and withstanding voltages of ±180 mV for up to tens of seconds. DPhPC was obtained from Avanti Polar Lipids, Inc. (Birmingham, AL), *n*-decane (99+% pure) was from Aldrich Chemical Co. (Milwaukee, WI), and tetrabutylammonium ($Bu_4N^+$) bromide (puriss) was purchased from Fluka Chemical Company (Ronkonkoma, NY).

Experiments were performed using a patch-clamp recorder (LIST EPC-7; Medical Systems Corp., Great Neck, NY) in voltage-clamp mode (50 GΩ feedback resistor) with a single pair of Ag/AgCl electrodes which made electrical contact with the solutions in the compartments via 3 M KCl agar salt bridges. The membrane conductance ($g$) in symmetric salt solutions is defined as the current ($I$) flowing through the membrane, divided by the transmembrane voltage ($V$); i.e., $g = I/V$, where $V$ is the potential of the *cis*, or toxin-containing, compartment relative to that of the *trans* compartment, which is taken as zero. Voltage stimuli were delivered to the clamp command input using a laboratory computer (Indec Systems, Sunnyvale, CA). Currents were filtered by the LIST clamp at 10 kHz (3-pole Bessel), digitized at 94 kHz with a 14-bit A/D recorder (model VR-10 digital data recorder; Instrutech Corp., Mineola, NY), and recorded and stored on VHS tape (Panasonic PV-2700 VCR) for subsequent playback and analysis. During the course of an experiment currents were displayed simultaneously on a strip chart recorder (General Scanning RS2-5P) and an oscilloscope (Hitachi V-212).

### *Determination of Mean Lifetimes in the Blocked and Unblocked States*

Data previously filtered at 10 kHz and stored in digital form on VHS tape were converted to analog (via Instrutech recorder), refiltered (typically at 2–8 kHz, −3 db) with an 8-pole tunable low-pass Bessel filter (model 902 LPF; Frequency Devices Inc., Haverhill, MA), and sampled (typically at 60 μs/point) using the Indec computer. Data were subsequently analyzed using a 50% threshold criterion to detect transitions (Sigworth, 1983), and a list of ~2,000 lifetimes in each of the open and closed states was generated. Histograms of these data were constructed using bins of constant width on a logarithmic time axis and fit with exponential probability density functions (pdf's) using a simplex routine that maximized log likelihood (Sigworth and Sine, 1987). We used log binning because it is more sensitive than traditional linear histograms at revealing multiple exponential processes (McManus et al., 1987; Sigworth and Sine, 1987), which would be present in our system if there were more than one binding site for $Bu_4N^+$ (see Fig. 1) and which were occasionally present as a result of contamination with "natural" flickering (see below).

To measure a significant number of blocking events (~2,000) at a given voltage, we generally needed to analyze 2–10 s of channel activity. We usually accomplished this by analyzing a continuous stretch of recording, a task made possible by the fact that, in the absence of blocker, the channel is, at most voltages, open for long periods of time. (At large negative voltages the channel is usually open for only a few seconds [see Results]; in these cases we sometimes had to pool data from different bursts.) However, when the channel is viewed at higher resolution in the absence of blocker, brief, rapid closures are evident (see Fig. 3). Although we have not made an extensive study of these kinetics, analysis at several voltages indicates that these rapid closures occur, on average, every 20 ms with a mean lifetime in the closed state of ~150 μs. These mean open and closed times varied ~50% from membrane to membrane, and showed no apparent voltage dependence. In the presence of $Bu_4N^+$ on either the *cis* or *trans* side of the membrane, and at most of the voltages studied, these natural closures were far outnumbered by sojourns to the blocked state, so that lifetimes in the closed

and open states were exponentially distributed—well fit by single-exponential pdfs (Fig. 2 *A*) with characteristic time constants representing the mean observed blocked time ($\tau_b^{obs}$) and unblocked time ($\tau_u^{obs}$), respectively.

As discussed below, the rate of blocking by $Bu_4N^+$ from the *cis* side is diffusion limited over most of the voltage range studied, so that with 15 $\mu$M $Bu_4N^+$ present in the *cis* solution the

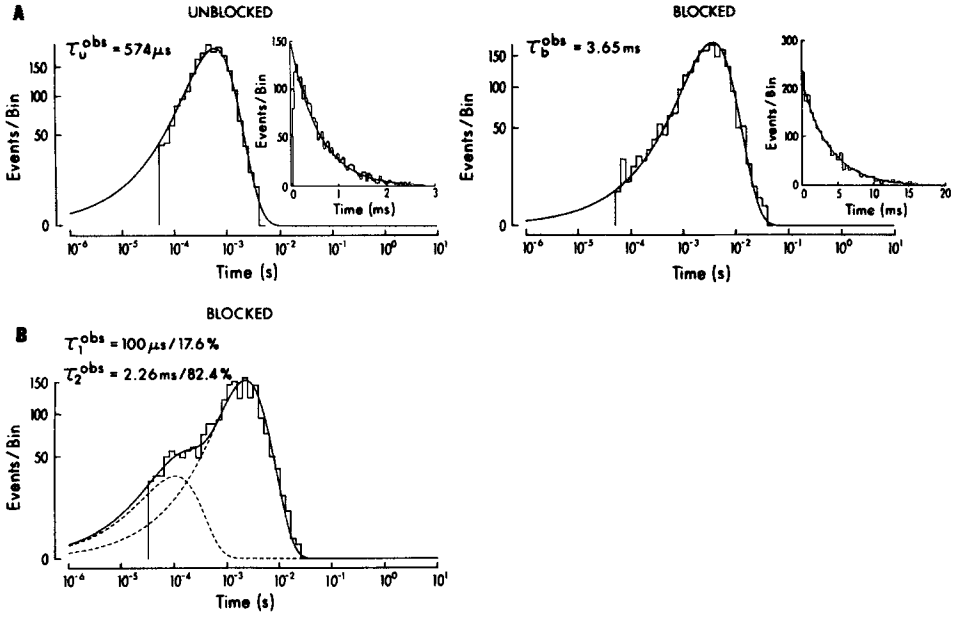


FIGURE 2. Histograms of the dwell times of the $PA_{65}$ channel in the blocked and unblocked states. Histograms were constructed and displayed using bins of constant width on a logarithmic time axis and fit with exponential pdfs using a simplex routine that maximized log likelihood; the ordinate is a square root scale (Sigworth and Sine, 1987). (The time constants [$\tau^{obs}$] obtained in this manner are displayed; they were subsequently corrected for missed events as discussed in Materials and Methods.) *A*, Representative histograms displaying single exponential pdfs. 2,040 blocked and unblocked events were analyzed from a continuous stretch of recording of a single channel in the presence of 15 $\mu$M $Bu_4N^+$ on the *cis* side ($V = +58$ mV). Data were filtered at 3.5 kHz and sampled at 60 $\mu$s/point. *Insets*, Standard linear histograms of the same data. The $\tau$'s used to draw the curves were those obtained from the above fits. *B*, Representative blocked-time histogram displaying a double exponential pdf. 2,075 blocked and unblocked events were analyzed from a continuous stretch of recording of a single channel in the presence of 2.5 mM $Bu_4N^+$ on the *trans* side ($V = +88$ mV). Data were filtered at 5 kHz and sampled at 60 $\mu$s/point. The solid curve is the sum of the two dashed curves representing the individual exponential components. (The histogram of the corresponding unblocked times [not shown] was fit by a single exponential pdf.)

mean unblocked time, $\tau_u$, varies only by about a factor of 3, with a minimum of ~450 $\mu$s (see Fig. 7). It was therefore sufficient, in generating data with $Bu_4N^+$ present in the *cis* solution, to probe the voltage range studied with a single concentration (15 $\mu$M) of $Bu_4N^+$. (We were limited at large negative voltages by the mean blocked time, $\tau_b$, which, by virtue of its voltage dependence, was <60 $\mu$s [our fastest sampling interval] at voltages less than −100 mV.) To

study blocking by $Bu_4N^+$ from the *trans* side, however, one concentration was not sufficient, because in the range −80 to +120 mV, $\tau_u$ increases three orders of magnitude (see Fig. 6). Therefore, we used lower concentrations of $Bu_4N^+$ ($\leq$200 $\mu$M) at negative voltages, so that $\tau_u$ would not be too fast, and higher concentrations ($\geq$1 mM) at positive voltages to insure that almost all of the closures would be due to blocking events rather than to the natural fast closures mentioned above. Even with this in mind, it was still not possible to avoid contamination by these events at all voltages and concentrations, and pdfs with two exponential components were occasionally observed (Fig. 2 *B*). Since, however, we believe that the process we are dealing with is, to a first approximation,

$$\text{closed} \underset{k_c}{\overset{k_o}{\rightleftharpoons}} \text{open} \underset{k_u}{\overset{k_b \cdot [Bu_4N^+]}{\rightleftharpoons}} \text{blocked},$$

filtering at 300 Hz eliminates 98% [1 − exp(0.60/0.15)] of these fast closures with 150 $\mu$s mean closed time ($\tau_c$). The observed time constants are then essentially those of the process

$$\text{open} \underset{k_u}{\overset{k_b \cdot [Bu_4N^+]}{\rightleftharpoons}} \text{blocked}$$

(after correcting for missed events as described below). This procedure works well when $\tau_b$ is at least a factor of 10 slower than $\tau_c$ (which was often the situation in our case), so that at least 70% of the blocking events are captured.

Because of finite filtering (1–8 kHz), and since under some conditions (at certain voltages and $Bu_4N^+$ concentrations) mean lifetimes are fairly short (<500 $\mu$s), a number of events failed to reach 50% threshold and were therefore "missed," causing $\tau_b^{obs}$ and $\tau_u^{obs}$ to be overestimates of the true time constants. Several strategies exist for calculating approximations to the true time constants from single-channel data (Sachs et al., 1982; Colquhoun and Sigworth, 1983; Neher, 1983; Blatz and Magleby, 1986), and although numerically complex, an exact solution to the general two-state problem has been derived (Roux and Sauvé, 1985). For accuracy and computational ease, we chose to correct for missed events using the nonlinear equations 79 and 80 in Colquhoun and Sigworth (1983),[1] which, after minor rearrangement, can be written in the form

$$\tau_u^{obs} = (\tau_u + \tau_b) \exp(t_d/\tau_b) - (\tau_b + t_d) \quad (1)$$

$$\tau_b^{obs} = (\tau_u + \tau_b) \exp(t_d/\tau_u) - (\tau_u + t_d), \quad (2)$$

and solved numerically. In these equations $t_d$ is the dead time of the recording system calculated according to the equation $t_d = 0.179/f_c$ (with $t_d$ in ms and $f_c$ in kHz), where $f_c$ is the −3-db filter frequency obtained from the equation for two Gaussian filters in series, $f_c^{-2} = f_1^{-2} + f_2^{-2}$ (Colquhoun and Sigworth, 1983). In our experiments $f_1$ is 10 kHz (LIST clamp) and $f_2$ is the filter setting used during playback. Corrections were typically <10% and at most 35%. Although we chose to analyze and display corrected data, our conclusions do not depend critically on these corrections.

[1] Blatz and Mableby (1986) have also addressed the problem of missed events in detail, and as they point out, their equations 7, 11, and 16 can be transformed into equations 79 and 80 of Colquhoun and Sigworth (1983).

## RESULTS

### *Qualitative Observations*

*Absence of $Bu_4N^+$.* Although we have not made a detailed investigation of the size and behavior of the $PA_{65}$ channel in the absence of blocking ions, as that is not the main focus of the present study, a few general properties are apparent. Channel conductance in 100 mM KCl usually ranges between 85 and 110 pS and is more or less ohmic between −160 and +160 mV. When viewed at low time resolution (10 Hz), channels open and close in a voltage-dependent fashion. At positive voltages channels are almost always open; however, at voltages ≥120 mV channels close with greater frequency but still stay open most of the time. With increasing negative voltages channels spend less time in the open state (seconds) and often stay closed for several seconds. This voltage dependence is consistent with the rapid fall of current seen when membranes containing many channels are stepped to large negative voltages (Blaustein et al., 1989). When viewed at higher time resolutions (>1 kHz), rapid, brief closures are evident (Fig. 3). Limited analysis of these closures reveals that they have an average duration of ~150 μs, occur with a frequency of ~50 Hz, and do not seem to be voltage dependent. Also sometimes seen is a channel of ~10 pS conductance, which may be a substate of the larger channel. Single-channel conductance is only weakly dependent on salt concentration between 10 and 200 mM KCl (35–110 pS); consequently, experiments in 100 mM KCl are near saturating concentrations of $K^+$.

*Presence of $Bu_4N^+$.* When added at micromolar concentrations to either the *cis* or *trans* solution, $Bu_4N^+$ induces a rapid on and off flickering of the channel that is strikingly voltage dependent; an example with $Bu_4N^+$ in the *cis* solution is shown in Fig. 3. The voltage dependence is consistent with $Bu_4N^+$ acting as a channel blocker: (*a*) At large negative voltages on the $Bu_4N^+$ side there is little flickering because the ion rarely enters the channel,[2] and once in the blocking site it quickly exits to the side from which it came. (*b*) At intermediate voltages there is rapid flickering as the ion enters and leaves the blocking site in the channel. (*c*) At large positive voltages there is still rapid flickering, but the channel spends little time in the "off" state, because although $Bu_4N^+$ frequently enters the blocking site it is quickly driven off the site and through the channel to the opposite solution. When viewed with low frequency resolution (0.5 Hz), the individual flickering events are not seen; instead, the apparent conductance of the channel first decreases, reaches a minimum, and then increases back towards its normal (unblocked) size, as the voltage of the $Bu_4N^+$ side is tromboned from −160 to +160 mV. What one is seeing is the mean proportion of time spent by the channel in the unblocked state. Plots of the *I-V* or *g-V* characteristic of the channel from filtered records are identical in shape to those obtained on membranes with many channels, confirming that the effects of tetraalkylammonium ions on the macroscopic *I-V* and *g-V* characteristics of $PA_{65}$-treated membranes, described in the previous paper (Blaustein and Finkelstein, 1990*a*), are

[2] This statement is more appropriate to the situation with $Bu_4N^+$ in the *trans* solution. As we shall see, its entry rate from the *cis* solution is only weakly voltage dependent.

a consequence of the voltage-dependent flickering induced by these ions on individual channels. (An example of this is seen in Fig. 4, where the ratio $\tau_u/(\tau_u + \tau_b)$ is plotted against voltage; this ratio equals the ostensible [normalized] conductance at low frequency resolution.)

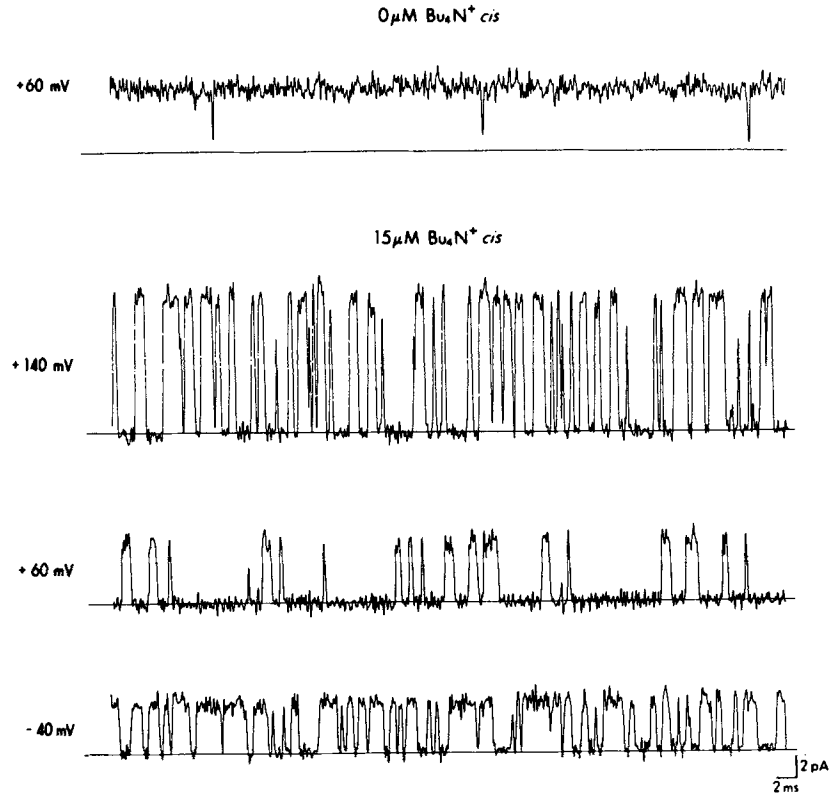


FIGURE 3. Single-channel records at a high time resolution in the absence and presence of 15 $\mu$M $Bu_4N^+$ in the *cis* solution. Data were filtered at 3 kHz and sampled at 60-$\mu$s intervals. The horizontal lines represent the closed or blocked state ($I = 0$); upward deflections are excursions to the open or unblocked state. Note that in going from $-40$ to $+60$ mV in the presence of $Bu_4N^+$ the dwell times in the blocked state increase, whereas in going from $+60$ to $+140$ mV they decrease. Dwell times in the unblocked state are relatively constant over this voltage range. Also note that in the absence of $Bu_4N^+$ there are only a few brief closures; although we show an example at only one voltage, it is typical of records seen at all voltages examined.

### *Quantitative Results*

*Closed times.* The distribution of times spent in the blocked state by a channel in the presence of $Bu_4N^+$ on one side of the membrane is described by a single exponential (e.g., Fig. 2 *A*) with a voltage-dependent time constant, $\tau_b$, whose value is independent both of the side on which $Bu_4N^+$ is present and of the $Bu_4N^+$

concentration (from 15 $\mu$M to 2.5 mM) (Fig. 5). These observables are consistent with a single binding site model as in Fig. 1.

The most significant aspect of the voltage dependence of $\tau_b$ (Fig. 5) is that the function goes through a maximum (at about $V = +60$ mV). This is the most convincing evidence that $Bu_4N^+$ (and by implication the other symmetric tetraalkylammonium blockers) can go through the channel. At negative and small positive voltages ($V < +20$ mV) the blocker almost always exits the channel to the *cis* side, whereas at large positive voltages ($V > +100$ mV) it almost always exits to the *trans* side; at intermediate voltages ($+20 < V < +100$ mV) there is a weighted probability of the blocker's exiting to either side. The semilogarithmic plot of $\tau_b$ vs. $V$ in Fig. 5 can be interpreted quantitatively in the above terms. Before doing this, however, we first analyze the open time behavior.

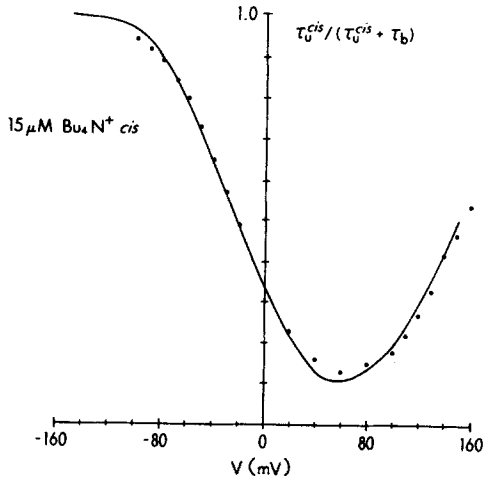


FIGURE 4. Comparison of fractional open time as a function of voltage from single-channel data (*dots*) to the normalized *g-V* relation of a many-channel membrane (*solid curve*). The data points are from a membrane containing a single channel, with 15 $\mu$M $Bu_4N^+$ in the *cis* solution, and represent the fraction of time spent by the channel in the unblocked state $[\tau_u^{cis}/(\tau_u^{cis} + \tau_b)]$. The solid curve (from Fig. 4 *B* of the preceeding paper [Blaustein and Finkelstein, 1990*a*]) is the normalized conductance (conductance in the presence of $Bu_4N^+$ divided by the conductance in its absence) obtained on a membrane containing thousands of channels, also with 15 $\mu$M $Bu_4N^+$ in the *cis* solution.

*Open times.* Like the blocked times, the open or unblocked times are also singly exponentially distributed (e.g., Fig. 2 *A*) with voltage-dependent time constants, $\tau_u^{cis}$ and $\tau_u^{trans}$ (where the superscripts identify the side of the membrane containing $Bu_4N^+$). As expected, the $\tau_u$'s are inversely proportional to the $Bu_4N^+$ concentration (from 15 $\mu$M to 2.5 mM [see Fig. 7 and especially Fig. 6]). It is therefore useful in discussing them to compare their values at a given concentration of $Bu_4N^+$, which we have chosen as 1 $\mu$M. For those who prefer second order rate constants (shown in Fig. 1) to time constants, the former are readily calculated from the latter through the relations:

$$k_1^{cis} = \frac{1}{[Bu_4N^+]^{cis} \cdot \tau_u^{cis}}$$

$$k_1^{trans} = \frac{1}{[Bu_4N^+]^{trans} \cdot \tau_u^{trans}}.$$

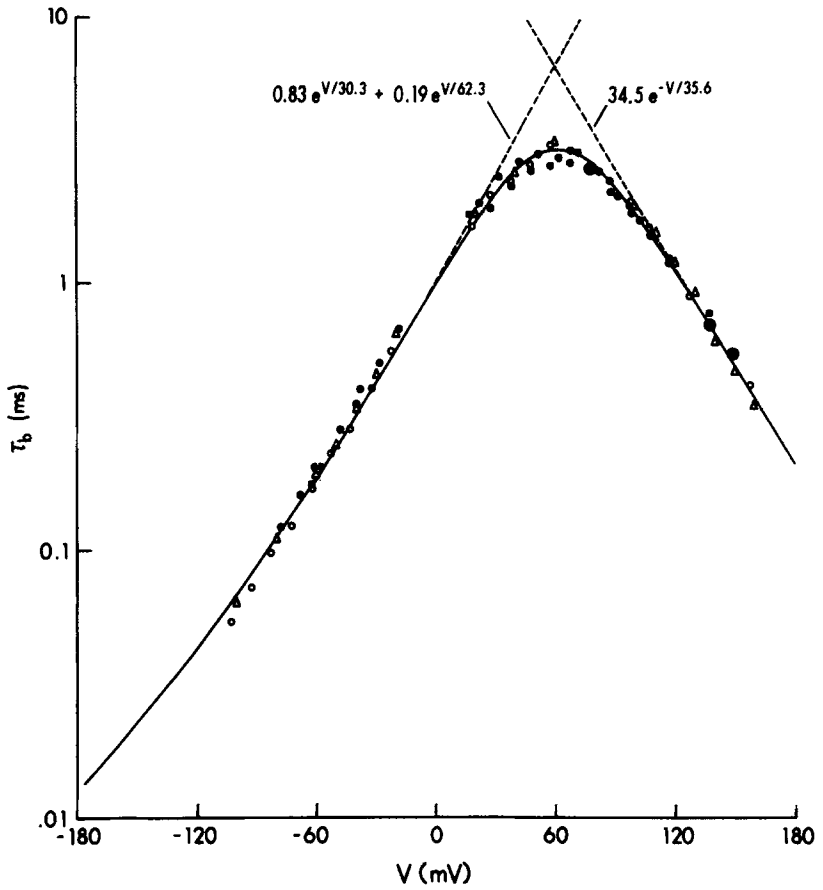


FIGURE 5. Semilogarithmic plot of the mean time ($\tau_b$) spent by a channel in the blocked state as a function of voltage. The open circles and the triangles are from two separate single-channel experiments with 15 $\mu$M $Bu_4N^+$ in the *cis* solution. (The solid squares are from the same experiment represented by the open circles, after the $Bu_4N^+$ concentration was raised to 37 $\mu$M.) The small solid dots are from several single-channel experiments with $Bu_4N^+$ present in the *trans* solution at concentrations ranging from 59 $\mu$M to 2.5 mM. (The large solid dots indicate that the data from the *cis* and *trans* experiments are identical at the resolution of the symbol size used.) The solid curve is Eq. 14 of the text:

$$\tau_b = [(0.83\,e^{V/30.3} + 0.189\,e^{V/62.3})^{-1} + (34.5\,e^{-V/35.6})^{-1}]^{-1}.$$

The dashed line,

$$\tau_b = 34.5\,e^{-V/35.6},$$

was fit by eye to the data points between +100 and +160 mV. The other dashed curve is Eq. 13 of the text and was derived as explained in the Appendix.

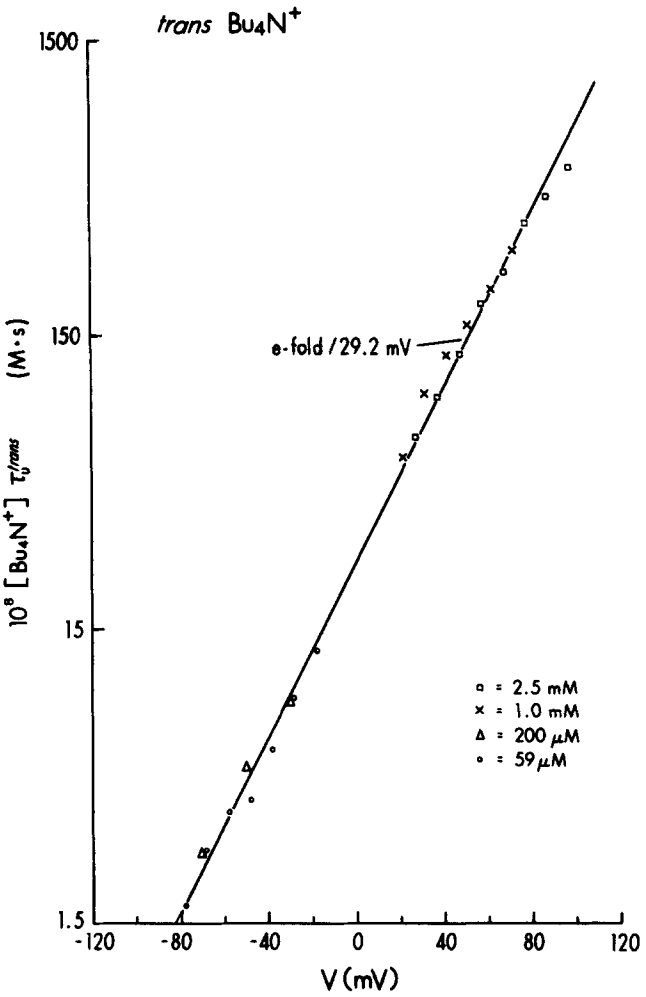


FIGURE 6. Semilogarithmic plot of the mean time ($\tau_u^{trans}$) spent by a channel in the unblocked state (times $[Bu_4N^+]$) as a function of voltage, with $Bu_4N^+$ in the *trans* solution. The experiments from which these mean unblocked times were obtained are the same experiments from which the mean blocked times in Fig. 5 (with $Bu_4N^+$ in the *trans* solution) were obtained. The straight line was fit by eye to the data points.

a. $Bu_4N^+$ on the *trans* side ($\tau_u^{trans}$). A semilogarithmic plot of $\tau_u^{trans}$ (times $[Bu_4N^+]$) vs. voltage yields a straight line with a slope corresponding to an *e*-fold change in $\tau_u^{trans}$ for every 29.2 mV (Fig. 6):

$$\tau_u^{trans} = 248\, e^{V/29.2}\ \text{ms} \qquad (\text{at } 1\ \mu\text{M})$$

or (3)[3]

$$k_1^{trans} = 4.03 \times 10^6\, e^{-V/29.2}\ \text{M}^{-1}\ \text{s}^{-1}.$$

[3] In all equations voltages are in millivolts.

That is, with $Bu_4N^+$ in the *trans* solution, the mean time that the channel spends unblocked increases *e*-fold for every 29.2-mV increase in voltage. This behavior has a simple interpretation in terms of the diagram in Fig. 1: the electrical distance from the *trans* solution to the *trans* energy barrier is 0.88 [$(kT/q)/29.2 = 25.6/29.2 = 0.88$].[4]

b. $Bu_4N^+$ on the *cis* side ($\tau_u^{cis}$). Whereas a semilogarithmic plot of $\tau_u^{trans}$ vs. voltage yields a straight line as seen in Fig. 6 and Eq. 3, a similarly simple relation for $\tau_u^{cis}$ does not exist. Fig. 7 shows a linear plot of $\tau_u^{cis}$ (times $[Bu_4N^+]$) vs. voltage. The voltage dependence of $\tau_u^{cis}$ is weak over most of the voltage range, becoming significant only for $V \leq -40$ mV; at large positive voltages, $\tau_u^{cis}$ plateaus to a value of about 6.75 ms (for $[Bu_4N^+] = 1$ $\mu$M).

How do we interpret this behavior? We believe that the rate at which $Bu_4N^+$ in the *cis* solution reaches the binding site within the channel is affected not only by the rate at which it moves in the electric field from the channel entrance to the binding site, but also by the rate at which it can diffuse (outside the electric field) from solution to the channel entrance. At large positive voltages this diffusion process becomes rate limiting and places a minimum value of 6.75 ms on $\tau_u^{cis}$ (for $[Bu_4N^+] = 1$ $\mu$M), which we shall call $\tau_u^{cis}$(diff):

$$\tau_u^{cis}(\text{diff}) = 6.75 \text{ ms} \quad (\text{at } 1\ \mu\text{M})$$

or (4)

$$k_1^{cis}(\text{diff}) = 1.48 \times 10^8\ \text{M}^{-1}\ \text{s}^{-1}.$$

At other voltages, $\tau_u^{cis}$(diff) contributes, along with the voltage-dependent component [$\tau_u^{cis}(V)$], to the overall value of $\tau_u^{cis}$. (Because of the larger energy barrier on the *trans* side [Fig. 1], the rate at which $Bu_4N^+$ from the *trans* side reaches the binding site is dominated [over the entire voltage range we studied] by the voltage-dependent kinetics of moving from the channel entrance to the site; hence diffusion from solution to the channel entrance does not make a significant contribution to $\tau_u^{trans}$.)[5] In the Discussion and the following paper (Blaustein and Finkelstein, 1990*b*) we offer several independent arguments for our assertion that the plateauing of $\tau_u^{cis}$ at large positive voltages is a consequence of diffusion limitation; for now, let us simply accept this.

Because the voltage-independent diffusion of $Bu_4N^+$ up to the channel entrance is in series with its subsequent voltage-dependent movement from the channel entrance to the binding site, it can readily be shown (see, for example, Schurr, 1970)

[4] In our analysis here and throughout the remainder of this paper we tacitly assume that the fraction of time that the binding site is occupied by the major current-carrying ion, $K^+$, is constant and is not a function of voltage. The near linear *I-V* characteristic of the channel in symmetric KCl offers some justification for this assumption, although the details of the argument are complicated and depend on how one models $K^+$ transport through the channel, a topic beyond the scope of this study.

[5] We do feel, however, that for $V < -100$ mV, diffusion limitation begins to significantly contribute to $\tau_u^{trans}$. This point is elaborated upon in the Discussion.

that:

$$\tau_u^{cis} = \tau_u^{cis}(\text{diff}) + \tau_u^{cis}(V). \tag{5}$$

Replotting the data in Fig. 7 as a semilogarithmic plot of $\tau_u^{cis} - \tau_u^{cis}(\text{diff})$ vs. voltage, we see (Fig. 8) that:

$$\tau_u^{cis}(V) = 1.53\, e^{-V/59}\ \text{ms} \quad (\text{at } 1\ \mu\text{M})$$

or (6)

$$k_1^{cis}(V) = 6.54 \times 10^8\, e^{V/59}\ \text{M}^{-1}\ \text{s}^{-1},$$

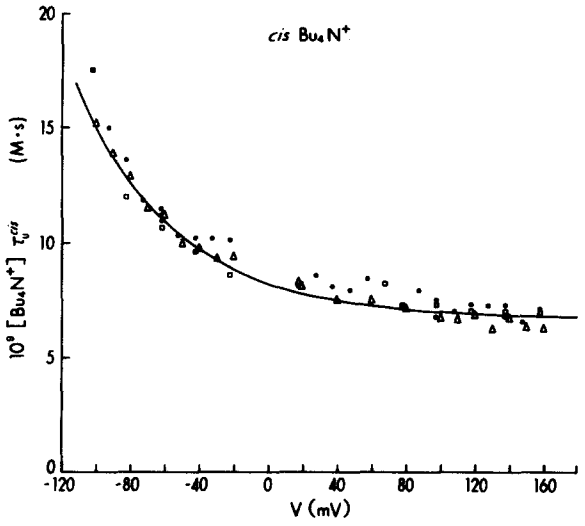


FIGURE 7. Linear plot of the mean time ($\tau_u^{cis}$) spent by a channel in the unblocked state (times $[Bu_4N^+]$) as a function of voltage, with $Bu_4N^+$ in the *cis* solution. The open circles, triangles, and squares are from three separate experiments in which the $Bu_4N^+$ concentration was 15 $\mu$M; two of these are the same two experiments from which the mean blocked times in Fig. 5 (with $Bu_4N^+$ in the *cis* solution) were obtained. (The solid and open circles are from the same experiment; solid circles represent data obtained after the $Bu_4N^+$ concentration was raised from 15 to 37 $\mu$M.) The curve is Eq. 7 (times $[Bu_4N^+]$) of the text.

which is analogous to Eq. 3 for $\tau_u^{trans}$. Combining this with Eqs. 4 and 5, we have for the complete expression for $\tau_u^{cis}$:

$$\tau_u^{cis} = 6.75\ \text{ms} + 1.53\, e^{-V/59}\ \text{ms} \quad (\text{at } 1\ \mu\text{M})$$

or (7)

$$k_1^{cis} = \frac{9.68\, e^{V/59}}{1.48 + 6.54\, e^{V/59}} \times 10^8\ \text{M}^{-1}\ \text{s}^{-1}.$$

This equation for $\tau_u^{cis}$ (times $[Bu_4N^+]$) provides a reasonable fit to the data in Fig. 7.

*The equation for $\tau_b$.* In terms of the diagram in Fig. 1, the exit rate constant ($k_{ex}$) of $Bu_4N^+$ from the binding site is given by the sum of the exit rate constants to the *cis* and *trans* solutions:

$$k_{ex} = k_{-1}^{cis} + k_{-1}^{trans}. \tag{8}$$

Calling $\tau_b^{cis}$ the dwell time in the blocked state if $Bu_4N^+$ could exit only to the *cis* solution, and $\tau_b^{trans}$ the dwell time in the blocked state if it could exit only to the *trans* solution, then since

$$\tau_b = \frac{1}{k_{ex}} \tag{9a}$$

$$\tau_b^{cis} = \frac{1}{(k_{-1}^{cis})} \tag{9b}$$

$$\tau_b^{trans} = \frac{1}{k_{-1}^{trans}}, \tag{9c}$$

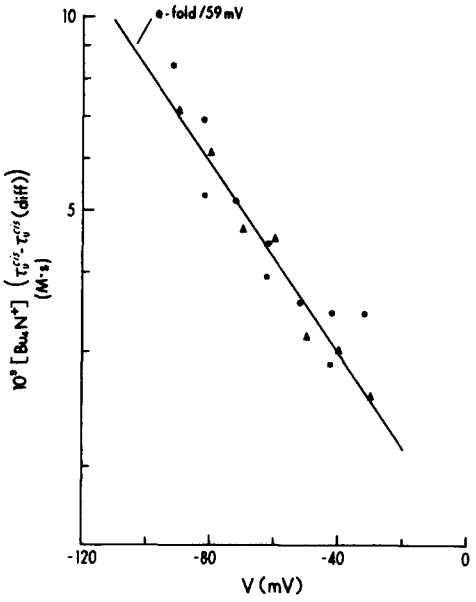


FIGURE 8. Semilogarithmic plot of $[\tau_u^{cis} - \tau_u^{cis}(\text{diff})]$ (times $[Bu_4N^+]$) as a function of voltage, with $Bu_4N^+$ in the *cis* solution. This is a replotting of the data points in Fig. 7. $[Bu_4N^+]$ $\tau_u^{cis}(\text{diff}) = 6.75 \times 10^{-9}$ M s (see Eq. 4). The straight line was fit by eye to the data points.

we have that:

$$\frac{1}{\tau_b} = \frac{1}{\tau_b^{cis}} + \frac{1}{\tau_b^{trans}}. \tag{10}$$

In the limit of large positive voltages (in practice, for $V \geq 100$ mV [see Fig. 5]) $Bu_4N^+$ will almost always exit to the *trans* side, and hence:

$$\tau_b \approx \tau_b^{trans} \quad (\text{for } V \geq 100 \text{ mV}). \tag{11a}$$

Similarly, in the limit of large negative voltages (in practice, for $V \leq 20$ mV [see Fig. 5])

$$\tau_b \approx \tau_b^{cis} \quad (\text{for } V \leq 20 \text{ mV}). \tag{11b}$$

We see from Fig. 5 that for $V \geq 100$ mV the data for $\tau_b$, in a semilogarithmic plot vs. voltage, are fit by a straight line, and from its slope and position we can write:

$$\tau_b^{trans} = 34.5\, e^{-V/35.6} \text{ ms.} \tag{12}$$

It would also seem that at negative voltages the data for $\tau_b$ in Fig. 5 can be similarly fit by a straight line. Although this perception is correct (by writing $\tau_b^{cis} = 1.15\, e^{V/36}$ and substituting it and Eq. 12 into Eq. 10, we obtain an expression for $\tau_b$ that excellently describes the data in Fig. 5), we feel it is conceptually wrong to represent $\tau_b^{cis}$ by a single exponential. The reason for this relates to the contribution of diffusion to $\tau_u^{cis}$ (see Eq. 7). Although the effect of diffusion on the *entrance* rate constant (and hence on $\tau_u^{cis}$) of $Bu_4N^+$ to the blocking site is easily conceived, there might appear at first glance to be no effect of diffusion on the *exit* rate constant, and hence on $\tau_b^{cis}$. It is well known, however, although not always appreciated, that if the forward rate constant of a reaction is affected by diffusion, then *by necessity* the reverse rate constant must be similarly affected. (A lucid presentation of the kinetic reasons for this can be found in the paper by Schurr [1970], and a further discussion of this point with respect to $Bu_4N^+$ block of the $PA_{65}$ channel is given in the accompanying paper [Blaustein and Finkelstein, 1990*b*]). As a consequence, $\tau_b^{cis}$ should be written not as a single exponential function of voltage but rather as the sum of two exponentials:

$$\tau_b^{cis} = 0.83\, e^{V/30.3} \text{ ms} + 0.188\, e^{V/62.3} \text{ ms.} \tag{13}$$

The analysis given in the Appendix discusses both why Eq. 13 is of this form and how we obtained the explicit expression for each term.

Substituting Eqs. 12 and 13 into Eq. 10 gives the complete expression for $\tau_b$:

$$\tau_b = [(0.83\, e^{V/30.3} + 0.189\, e^{V/62.3})^{-1} + (34.5\, e^{-V/35.6})^{-1}]^{-1} \text{ ms,} \tag{14}$$

which provides an excellent fit to the data points in Fig. 5.

## DISCUSSION

As recounted in the preceding paper (Blaustein and Finkelstein, 1990*a*), symmetric tetraalkylammonium ions added at micromolar concentrations to either the *cis* or *trans* solutions produce dramatic voltage-dependent effects on the "instantaneous" *g-V* characteristics of planar phospholipid bilayer membranes containing hundreds or thousands of channels formed by the $PA_{65}$ fragment of anthrax toxin. We postulated that the effects resulted from a voltage-dependent block of the channels by these ions to the major current-carrying potassium ion (present at a concentration of 100 mM). In this paper we investigated in detail the action of one of these ions, tetrabutylammonium ($Bu_4N^+$), at the single-channel level. Our interpretation of the experimental data, which accompanied to some extent the presentation of the results, has been in terms of the free energy diagram of the channel shown in Fig. 1, which consists of a single well (or blocking site) for the ion, situated between two barriers. As we shall see, this model accounts quantitatively for the action of $Bu_4N^+$ and also allows us to draw inferences about channel structure and size.

*Agreement of Single-Channel and Macroscopic Results*

Before analyzing the single-channel results, we note that they are in complete accord with the macroscopic results obtained previously with $Bu_4N^+$ on membranes containing many channels (Blaustein and Finkelstein, 1990*a*) and that therefore the single $PA_{65}$ channels studied here are representative of the whole. A plot vs. voltage of the fraction of the time that the channel is open or unblocked $[\tau_u/(\tau_u + \tau_b)]$, where $\tau_u$ and $\tau_b$ are the mean times spent in the unblocked and blocked states, respectively, coincides with the normalized conductance vs. voltage curve for a many-channel membrane (e.g., Fig. 4). The fall of macroscopic conductance in going from negative to positive voltages (on the $Bu_4N^+$ side), followed by its subsequent rise at larger positive voltages, is paralleled at the single-channel level by the fraction of time that the channel spends unblocked.

*Consistency of Single-Channel Data with the Two-Barrier, One-Well Model*

There are three obligatory mathematical consequences of the single-well (or site) model in Fig. 1 with respect to the mean time that the channel stays blocked: (*a*) the distribution of times spent by the channel in the blocked state at a given voltage must be described by a single exponential (with a characteristic time constant, $\tau_b$); (*b*) $\tau_b$ must be independent of the side of the membrane from which $Bu_4N^+$ entered the channel; and (*c*) $\tau_b$ must be independent of the $Bu_4N^+$ concentration. All three of these consequences are met by the experimental data (see especially Fig. 5). Although more baroque energy diagrams can be imagined that would predict consequences experimentally indistinguishable from the above three, the single-well model is by far the simplest.

Since $\tau_b$ is independent of the side from which $Bu_4N^+$ entered the blocking site, the ~30-fold higher concentration of $Bu_4N^+$ required from the *trans* as compared with the *cis* side to produce a given decrease in conductance (at $V = 0$) in macroscopic experiments (Blaustein and Finkelstein, 1990*a*) must be reflected in the unblocked times, $\tau_u$'s. From Figs. 6 and 7 (or comparing Eq. 3 with Eq. 7) we see indeed that at $V = 0$, an ~30-fold higher concentration of $Bu_4N^+$ is required from the *trans* side to achieve the same value of $\tau_u$ obtained with $Bu_4N^+$ from the *cis* side. In the two-barrier, single-well model drawn in Fig. 1, this fact is reflected in the greater height of the *trans* barrier. In other words, for a given concentration of $Bu_4N^+$, its entry rate at $V = 0$ from the *trans* side ($k_1^{trans}$) is ~30-fold slower than that from the *cis* side ($k_1^{cis}$). Also consistent with the two-barrier, single-well model (although equally consistent with almost any other reasonable model) is our finding that the times spent in the unblocked state are singly exponentially distributed, and the $\tau_u$'s are inversely proportional to the $Bu_4N^+$ concentration (see especially Fig. 6).

*Interpretation of the Voltage Dependencies of the Time Constants*

*The mean blocked time ($\tau_b$).* The most reasonable, and virtually compelling, interpretation of the maximum at about +60 mV in the $\tau_b$ vs. $V$ curve (Fig. 5) is that for $V \leq 20$ mV, a $Bu_4N^+$ at the blocking site almost always exits to the *cis* solution, whereas for $V \geq 100$ mV it almost always exits to the *trans* solution. At intermediate voltages the probability of exiting to the *cis* or *trans* solution is $k_{-1}^{cis}/(k_{-1}^{cis} + k_{-1}^{trans})$ or

$k_{-1}^{trans}/(k_{-1}^{cis} + k_{-1}^{trans})$, respectively, where the $k$'s are defined in Fig. 1. (We shall comment further on the voltage dependence of $\tau_b$ in our discussion of the voltage dependencies of the $\tau_u$'s).

Short of a direct chemical determination of the appearance of $Bu_4N^+$ in the compartment opposite that to which it was added, the maximum in its $\tau_b$ vs. $V$ curve is the most direct evidence that $Bu_4N^+$ can traverse the channel, an assumption we made from the existence of a minimum in the macroscopic $g$-$V$ curve with $Bu_4N^+$ in one solution (Blaustein and Finkelstein, 1990*a*). (A maximum in mean blocked time is also seen with suberyldicholine block of acetylcholine receptor channels [Sine and Steinbach, 1984] and with divalent ion block of calcium channels [Lansman et al., 1986].) Similar minima are observed in the macroscopic $g$-$V$ curves for tetrapentylammonium and tetrahexylammonium ion block (Blaustein and Finkelstein, 1990*a*) and in filtered single-channel records with tetraheptylammonium ion (data not shown); these observations imply that the above ions can also traverse the channel. Since tetraheptylammonium ion has a diameter of ~12 Å (Robinson and Stokes, 1959), the channel diameter must be at least this large at its narrowest point.[6]

*The mean unblocked time ($\tau_u$).* a. $Bu_4N^+$ present in the *trans* solution ($\tau_u^{trans}$). $\tau_u^{trans}$ manifests a simple exponential dependence on voltage with a steepness of $e$-fold per 29.2 mV (Fig. 6 and Eq. 3). This means, as noted in the Results section, that the electrical distance from the *trans* solution to the *trans* energy barrier is 0.88. At large positive voltages, when $Bu_4N^+$ almost always exits to the *trans* solution, $\tau_b^{trans}$ (i.e., the value of $\tau_b$ when $Bu_4N^+$ exits only to the *trans* solution) also manifests a simple exponential dependence on voltage, in this case with a steepness of $e$-fold per 35.6 mV (Eq. 12). This means, in terms of the same energy diagram, that the electrical distance from the binding site to the *trans* energy barrier is 0.72. Three inferences can be drawn from these observations: (*a*) since $\tau_u^{trans}$ and $\tau_b^{trans}$ have approximately equally steep voltage dependencies (29.2 and 35.6 mV, respectively), the energy barrier is (electrically) roughly midway between the *trans* solution and the blocking site; (*b*) the voltage dependence of $e$-fold per 16 mV ($e^{V/29.2}/e^{-V/35.6}$) for the free energy of $Bu_4N^+$ at the binding site with respect to the *trans* solution is in excellent agreement with the value of $e$-fold per 17 mV obtained from macroscopic experiments (Blaustein and Finkelstein, 1990*a*); (*c*) the electrical distance of 1.6 (0.88 + 0.72) from the *trans* solution to the binding site implies that on average there are ~1.6 ions in the channel between the *trans* side and the blocking site; that is, in the absence of $Bu_4N^+$ there are on average 1.6 potassium ions in this region of the channel.

b. $Bu_4N^+$ present in the *cis* solution ($\tau_u^{cis}$). In contrast to $\tau_u^{trans}$, $\tau_u^{cis}$ does not display the simple exponential dependence on voltage that is anticipated from the energy diagram in Fig. 1. Over most of the voltage range studied it is weakly voltage dependent, and plateaus (at large positive voltages) to a voltage-independent value of 6.75 ms (for $[Bu_4N^+] = 1\ \mu M$). As indicated in the Results, we believe that this is because $\tau_u^{cis}$ is diffusion limited by the rate at which $Bu_4N^+$ can get from the *cis* solution to the channel entrance.

[6] It is conceivable that the alkyl tails of the ions we have studied can insinuate themselves in hydrophobic regions of the channel wall, and that therefore the channel "diameter" available to these ions is larger than that available to more hydrophilic molecules.

There are two arguments that we can offer at this juncture to support this belief (further arguments are given in the following paper [Blaustein and Finkelstein, 1990*b*]). First, voltage independence of $\tau_u^{cis}$ (at large positive voltages) means that the rate-limiting step is occurring in a region that does not sense the electric field. The solution near the channel entrance, which $Bu_4N^+$ must traverse before entering the channel, is such a voltage-insensitive region. Second, the plateau value of $\tau_u^{cis}$ is consistent with diffusion limitation. A value for $\tau_u^{cis}$ of 6.75 ms at 1 $\mu$M $Bu_4N^+$ translates to a second order rate constant for $k_1^{cis}$ in Fig. 1 of $1.48 \times 10^8\ M^{-1}\ s^{-1}$. For a disk of capture radius $r_c$, the diffusion-limited rate constant is equal to

$$k_1^{cis}(\text{diff}) = 4DN_A r_c, \tag{15}$$

where $D$ is the diffusion constant of $Bu_4N^+$ and $N_A$ is Avagadro's number (see Berg, 1983). If the radius of the channel is ~6 Å (which we infer from its permeability to tetraheptylammonium ion) and the radius of $Bu_4N^+$ is ~5 Å (Robinson and Stokes, 1959), the capture radius is ≈1 Å. Taking $D$ is $\sim 5.3 \times 10^{-6}\ cm^2/s$ (calculated from the data in Robinson and Stokes [1959]), we then have from Eq. 15 the diffusion-limited rate constant:

$$k_1^{cis}(\text{diff}) \approx 1.3 \times 10^8\ M^{-1}s^{-1} \qquad \text{(theoretical)},$$

which is in very good agreement with our experimental value for $k_1^{cis}$ of $1.48 \times 10^8\ M^{-1}s^{-1}$ (Eq. 4). The representation of the pore entrance as a disk of radius 6 Å, assigning the capture radius of $Bu_4N^+$ a value of 1 Å (because its radius is 5 Å), and applying these values to Eq. 15 are highly idealized approximations to the diffusion-limited rate of entry of $Bu_4N^+$ into the channel. Consequently, the excellent agreement of the experimental and theoretical values of $k_1^{cis}$(diff) is undoubtedly fortuitous; we mention it merely to show that the magnitude of the plateau value of $\tau_u^{cis}$ is consistent with diffusion limitation.

At very large negative voltages where the movement of $Bu_4N^+$ in the electric field from the channel entrance to the binding site is slow compared with its rate of diffusion from the *cis* solution up to the channel entrance, the voltage-dependent component of $\tau_u^{cis}$ is proportional to $e^{-V/59}$ (Eq. 6). Since the voltage dependence of the free energy of $Bu_4N^+$ at the binding site with respect to the *cis* solution is $e$-fold per 30.3 mV (Eq. A3), at large negative voltages the *cis* barrier is approximately midway between the *cis* solution and the binding site.[7] The total electrical distance from the binding site to the *cis* solution is 0.84 [$(kT/q)/30.3 = 25.6/30.3 = 0.84$], which means that on average (in the absence of $Bu_4N^+$) there is about one potassium ion in the channel between the *cis* solution and the binding site. If we combine this with the 1.6 potassium ions between the *trans* solution and the binding site, we conclude that in 100 mM KCl the $PA_{65}$ channel contains two to three potassium ions, a conclusion that we also reached from the analysis of the macroscopic $g$-$V$ curve (Blaustein and Finkelstein, 1990*a*).

[7] A diffusion "barrier" cannot be incorporated in a simple way into the barrier scheme depicted in Fig. 1. In a formal sense, the position of the barrier moves from approximately midway between the channel entrance and the binding site at large negative voltages (where $\tau_u^{cis}$ is totally diffusion independent), to the channel entrance at large positive voltages (where $\tau_u^{cis}$ is totally diffusion limited).

### *The Mathematical Reason for the Minimum in the Macroscopic g-V Characteristic*

In the previous paper (Blaustein and Finkelstein, 1990*a*) we found that with $Bu_4N^+$ present in the *cis* solution, there is a minimum in the macroscopic *g-V* curve at about +60 mV, and with $Bu_4N^+$ present in the *trans* solution the minimum occurs at about −60 mV. How are these observables explained at the single-channel level?

The minimum at +60 mV with $Bu_4N^+$ in the *cis* solution is easily understood. Since $\tau_u^{cis}$ is virtually voltage independent over most of the range studied, the voltage dependence of the macroscopic conductance (which is proportional to $\tau_u^{cis}/[\tau_u^{cis} + \tau_b]$) simply reflects the voltage dependence of $\tau_b$. Since $\tau_b$ reaches a maximum at about +60 mV (Fig. 5), the macroscopic conductance ($g$) attains a minimum at this value.

The reason for the minimum at −60 mV with $Bu_4N^+$ in the *trans* solution is not as obvious. As mentioned previously, a plot vs. voltage of the filtered single-channel conductance in the presence of *trans* $Bu_4N^+$ (normalized to the conductance in the absence of $Bu_4N^+$) yields a curve that is nearly identical to the normalized *g-V* curve generated from macroscopic data. The important feature of these curves is that they exhibit a minimum at approximately −60 mV, consistent with relief of block at voltages more negative than −60 mV. (It is difficult to generate this region of the curve using the actual mean lifetimes, $\tau_u^{trans}$ and $\tau_b$, since for voltages ≤ −100 mV, $\tau_b$ becomes too fast [<60 μs] to measure reliably.) If, however, we generate a theoretical normalized *g-V* curve using Eqs. 3 and 14 for $\tau_u^{trans}$ [8] and $\tau_b$, respectively, we find that the function $\tau_u^{trans}/[\tau_u^{trans} + \tau_b]$ does not have a minimum, but instead decreases monotonically with decreasing voltage. The function fits the data well for voltages greater than 0 mV, but poorly for voltages less than −60 mV. If a constant term, ranging from 0.012 to 0.030 ms,[9] is added to $\tau_u^{trans}$ above, the resulting function does display a minimum, and in fact looks somewhat similar to the actual data. Although we have not analyzed this in detail, these crude simulations suggest that relief of block at voltages less than −60 mV may result from diffusion limitation contributing to $\tau_u^{trans}$ in this voltage range. Our data for $\tau_u^{trans}$ do not show evidence of diffusion limitation, as the semilogarithmic plot of $\tau_u^{trans}$ (times $[Bu_4N^+]$) vs. $V$ is fairly linear (Fig. 6). It is possible, however, that since it is difficult to determine time constants at large negative voltages (for reasons discussed above), we have missed a small deviation from linearity in this voltage range.

## APPENDIX

### *Derivation of the Expression for $\tau_b^{cis}$ Given in Eq. 13*

Imagine that the *trans* barrier in Fig. 1 is so large that at all voltages a $Bu_4N^+$ at the blocking site can exit only to the *cis* solution. Thus, $Bu_4N^+$ in the *cis* solution is essentially in equilibrium with $Bu_4N^+$ at the blocking site. (Since $K^+$ can still flow through the unblocked channel, this is not a true equilibrium system, but it is a reasonable approximation to analyze the behavior of $Bu_4N^+$ from equilibrium arguments. A true equilibrium would pertain to a system in which no

[8] This term was scaled to 250 μM for comparison with actual data.

[9] This would correspond to a range of 3.0–7.5 ms at a concentration of 1 μM.

ion could traverse the channel, in which case we would simply be dealing with the binding of $Bu_4N^+$ to a site.) The ratio of the time spent by the channel in the unblocked state ($\tau_u^{cis}$) (times $[Bu_4N^+]$) to the time spent in the blocked state ($\tau_b^{cis}$) is then represented by a voltage-dependent equilibrium constant ($K_{eq}$) of the form

$$K_{eq} = \frac{k_{-1}^{cis}}{k_1^{cis}} = \frac{[Bu_4N^+]\tau_u^{cis}}{\tau_b^{cis}} = Ae^{-V/a}. \quad \text{(A1)}$$

At negative voltages $Bu_4N^+$ actually exits the blocking site almost exclusively to the *cis* solution, so that Eq. A1 is applicable to this case. From the plot of $[Bu_4N^+]\tau_u^{cis}/\tau_b$ vs. $V$ in Fig. 9 we can therefore write an explicit expression for Eq. A1:

$$K_{eq} = \frac{k_{-1}^{cis}}{k_1^{cis}} = \frac{[Bu_4N^+]\tau_u^{cis}}{\tau_b^{cis}} = 8.1 \times 10^{-6}\, e^{-V/30.3}\ \text{M} \quad \text{(A2a)}$$

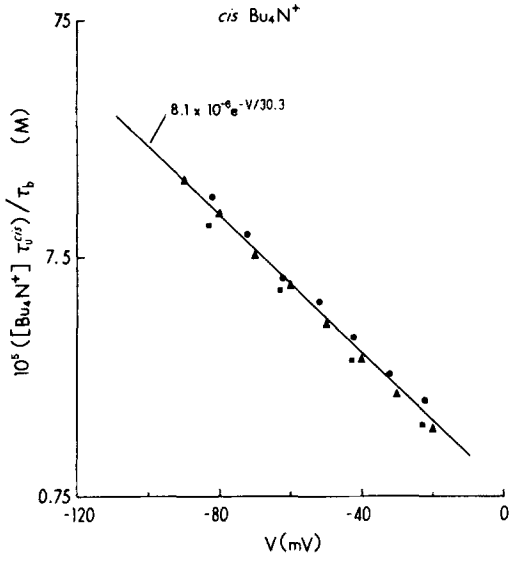


FIGURE 9. Semilogarithmic plot of the ratio of the mean unblocked time ($\tau_u^{cis}$) (times $[Bu_4N^+]$) to the mean blocked time ($\tau_b$) as a function of voltage. The values used for $[Bu_4N^+]\tau_u^{cis}$ are from Fig. 7 and the values for $\tau_b$ are from the corresponding experiments in Fig. 5; only data in the voltage range $-20$ to $-100$ mV are used. The straight line was fit by eye to the data points.

or

$$\tau_b^{cis} = [Bu_4N^+]\tau_u^{cis}(1.23 \times 10^5\, e^{V/30.3})\ \text{ms}. \quad \text{(A2b)}$$

Let us now consider two limiting cases. At large positive voltages $\tau_u^{cis}$ is diffusion limited and approaches 6.75 ms for $[Bu_4N^+] = 1\ \mu$M, which is $\tau_u^{cis}$(diff) (see Eq. 7). Thus, from Eq. A2b we have

$$\tau_b^{cis} = 0.83\, e^{V/30.3}\ \text{ms} \quad \text{(for large positive voltages)}. \quad \text{(A3)}$$

For large enough negative voltages, $\tau_u^{cis}$ is totally dominated by its voltage-dependent component, and diffusion makes a negligible contribution to its value. This is seen formally in Eq. 7, from which we get

$$\tau_u^{cis} = 1.53\, e^{-V/59}\ \text{ms} \quad \text{(for large negative voltages, } [Bu_4N^+] = 1\ \mu\text{M}),$$

and substituting this into Eq. A2b, we obtain

$$\tau_b^{cis} = 0.188\, e^{V/62.3}\ \text{ms} \quad \text{(for large negative voltages)}. \tag{A4}$$

Thus, as $\tau_u^{cis}$ (or $k_1^{cis}$) moves with voltage from its voltage-independent, diffusion-limited value to one that is totally voltage dependent, the steepness of the voltage dependence of $\tau_b^{cis}$ changes from a proportionality of $e^{V/30.3}$ (Eq. A3) to $e^{V/62.3}$ (Eq. A4). The thermodynamic reason for this is that when $\tau_u^{cis}$ (or $k_1^{cis}$) is diffusion limited and is not voltage dependent, all of the voltage dependence in $K_{eq}$ of Eq. A2a resides in $\tau_b^{cis}$ (or $k_{-1}^{cis}$), whereas when $\tau_u^{cis}$ is voltage dependent, $\tau_b^{cis}$ shares the voltage dependence of $K_{eq}$ with $\tau_u^{cis}$ and hence is less steeply voltage dependent. The kinetic reason for this is not so obvious, and the interested reader should consult Schurr (1970). Analogous to Eq. 5, in which $\tau_u^{cis}$ is the sum of $\tau_u^{cis}$(diff) and $\tau_u^{cis}(V)$, it turns out that the same relation exists between $\tau_b^{cis}$ and its limiting conditions (Schurr, 1970). Thus, from Eqs. A3 and A4 we can write the general expression for $\tau_b^{cis}$

$$\tau_b^{cis} = 0.83\, e^{V/30.3}\ \text{ms} + 0.188\, e^{V/62.3}\ \text{ms},$$

which is Eq. 13 of the text. For $V \leq 20$ mV, $\tau_b \approx \tau_b^{cis}$ (Eq. 11b), and Eq. 13 indeed fits our data for $V \leq 20$ mV. It is amusing that between $-100$ and $+20$ mV, where all our data points that are fit by Eq. 13 lie, Eq. 13 is almost indistinguishable from a single exponential function

$$\tau_b^{cis} = 1.15\, e^{V/36}\ \text{ms},$$

which fits our data equally well.

We are grateful to Dr. William F. Wonderlin for teaching us his elegant techniques for forming low noise bilayers, and we thank Dr. Fred Sigworth and Dr. Steve Sine for advice on single-channel recording methodology and for generously providing the computer programs used for analysis. We also thank Dr. Olaf Andersen and Dr. Christopher Miller for helpful discussions and for critically reading this manuscript.

This work was supported by NIH Medical Scientist training grant T32GM7288 from NIGMS to R. O. Blaustein and by NIH grant GM-29210-12 to A. Finkelstein.

*Original version received 28 December 1989 and accepted version received 17 April 1990.*

## REFERENCES

Berg, H. C. 1983. Random Walks in Biology. Princeton University Press, Princeton, NJ. 26–28.

Blatz, A. L., and K. L. Magleby. 1986. Correcting single channel data for missed events. *Biophysical Journal.* 49:967-980.

Blaustein, R. O., and A. Finkelstein. 1990*a*. Voltage-dependent block of anthrax toxin channels in planar phospholipid bilayer membranes by symmetric tetraalkylammonium ions. Effects on macroscopic conductance. *Journal of General Physiology.* 96:905–919.

Blaustein, R. O., and A. Finkelstein. 1990*b*. Diffusion limitation in the block by symmetric tetraalkylammonium ions of anthrax toxin channels in planar phospholipid bilayer membranes. *Journal of General Physiology.* 96:943–957.

Blaustein, R. O., T. M. Koehler, R. J. Collier, and A. Finkelstein. 1989. Anthrax toxin: channel-forming activity of protective antigen in planar phospholipid bilayers. *Proceedings of the National Academy of Sciences USA.* 86:2209–2213.

Colquhoun, D., and F. J. Sigworth. 1983. Fitting and statistical analysis of single-channel records. *In* Single-Channel Recording. B. Sakmann and E. Neher, editors. Plenum Publishing Corporation, New York. 191–263.

Lansman, J. B., P. Hess, and R. W. Tsien. 1986. Blockade of current through single calcium channels by $Cd^{2+}$, $Mg^{2+}$, and $Ca^{2+}$. Voltage and concentration dependence of calcium entry into the pore. *Journal of General Physiology.* 88:321–347.

McManus, O. B., A. L. Blatz, and K. L. Magleby. 1987. Sampling, log binning, fitting, and plotting durations of open and shut intervals from single channels and the effects of noise. *Pflügers Archiv.* 410:530–553.

Mueller, P., D. O. Rudin, H. T. Tien, and W. C. Wescott. 1963. Methods for the formation of single bimolecular lipid membranes in aqueous solution. *Journal of Physical Chemistry.* 67:534–535.

Neher, E. 1983. The charge carried by single-channel currents of rat cultured muscle cells in the presence of local anaesthetics. *Journal of Physiology.* 339:663–678.

Robinson, R. A., and R. H. Stokes. 1959. Electrolyte Solutions. 2nd ed. Butterworth & Co., Ltd., London. 1–571.

Roux, B., and R. Sauvé. 1985. A general solution to the time interval omission problem applied to single channel analysis. *Biophysical Journal.* 48:149–158.

Sachs, F., J. Neil, and N. Barkakati. 1982. The automated analysis of data from single ionic channels. *Pflügers Archiv.* 395:331–340.

Schurr, J. M. 1970. The role of diffusion in bimolecular solution kinetics. *Biophysical Journal.* 10:700–716.

Sigworth, F. J. 1983. An example of analysis. *In* Single-Channel Recording. B. Sakmann and E. Neher, editors. Plenum Publishing Corporation, New York. 301–321.

Sigworth, F. J., and S. M. Sine. 1987. Data transformations for improved display and fitting of single-channel dwell time histograms. *Biophysical Journal.* 52:1047–1054.

Sine, S.M., and J.H. Steinbach. 1984. Agonists block currents through acetylcholine receptor channels. *Biophysical Journal.* 46:277–284.

Wonderlin, W. F., A. Finkel, and R. J. French. 1990. Optimizing planar lipid bilayer single-channel recordings for high resolution with rapid voltage steps. *Biophysical Journal.* 58:289–297.